

# Exploring evidence of interaction between dark energy and dark matter

Daniela Grandón\* and Víctor H. Cárdenas†

*Instituto de Física y Astronomía, Facultad de Ciencias,  
Universidad de Valparaíso, Av. Gran Bretaña 1111, Valparaíso, Chile*

(Dated: October 23, 2018)

## Abstract

In this work we use the latest observations on SNIa,  $H(z)$ , BAO,  $f_{gas}$  in clusters and CMBR, to constrain three models showing an explicit interaction between dark matter and dark energy. In particular, we use the BOSS BAO measurements at  $z \simeq 0.32$ , 0.57 and 2.34, using the full 2-dimensional constraints on the angular and line of sight BAO scale. We find that using all five observational probes together, two of the interaction models show positive evidence at more than  $3 \sigma$ . Although significant, further study is needed to establish this statement firmly.

---

\*Electronic address: daniela.grandon@alumnos.uv.cl

†Electronic address: victor.cardenas@uv.cl

## I. INTRODUCTION

One of the most important problems of theoretical physics is to explain the fact that the universe is in a phase of accelerated expansion. Since 1998 [1], [2], the physical origin of cosmic acceleration remains a deep mystery. According to general relativity (GR), if the universe is filled with ordinary matter or radiation, the two known constituents of the universe, gravity should slow the expansion. Since the expansion is speeding up, we are faced with two possibilities, either of which would have profound implications for our understanding of the cosmos and of the laws of physics. The first is that 75% of the energy density of the universe exists in a new form with large negative pressure, called dark energy (DE) [3], [4], [5]. The other possibility is that GR breaks down on cosmological scales and must be replaced with a more complete theory of gravity [6]. In this paper we consider the first option. The cosmological constant, the simplest explanation of accelerated expansion, has a checkered history [7], [8], having been invoked and subsequently withdrawn several times before. In quantum field theory, we estimate the value of the cosmological constant as the zero-point energy with a short-cut scale, for example the Planck scale, which results in an excessively greater value than the observational results.

Although the  $\Lambda$ CDM model has been confirmed as the one that best fits all the observational tests [28], in recent years the precision of measurements and the increase in the number of them have led to a model *extension* being seriously considered [10]. Among the different ways in which we can deform the  $\Lambda$ CDM model are:

(i) To propose models where the cosmological constant is dynamic, i.e. it changes with time. This family includes the models of quintessence, for example, and from which comes the name *dark energy*, which is interpreted as a contribution to the matter content of the universe, the nature of which is unknown.

(ii) Models where the gravitational theory is modified, i.e., it is expected to account for the effect of the cosmological constant.

(iii) Models where one of the fundamental principles of cosmology is relaxed, which is the homogeneity, openly violating the Copernican principle.

One of the type (i) models that has received much attention in recent years is the model of interaction between dark matter (DM) and DE [11], [12], [13], [14]. Since we do not know the nature of DM (non-baryonic) and DE, it is not unreasonable to assume that the two may

be related. An exploratory form in which this occurs is by assuming that there is a small transfer of energy among DE and DM, modeled as a small coupling because the concordance model – a cosmological constant plus DM – is a good fit to the data. This scenario, a direct interaction between these dark contributions appears as an observational viable option [15].

The interaction is usually modeled phenomenologically by modifying the conservation equations through a  $Q$  function,

$$\begin{aligned}\dot{\rho}_c + 3H\rho_c &= Q, \\ \dot{\rho}_d + 3H(1 + \omega)\rho_d &= -Q,\end{aligned}\tag{1}$$

where  $\rho_d$  is the DE density,  $\rho_c$  the DM component, in such a way that only the sum of the contributions is conserved, but not each one separately. If  $Q < 0$  there is an energy transfer from DM to DE, and the opposite occurs for  $Q > 0$ . Although the sign of  $Q$  is not defined from first principles, there are arguments in favor of an overall transfer of energy from DE to DM [16], [17],[18] and also in the other way [19], [20] with also some works indicating a redshift dependence in the sign of  $Q$  [21]. Mention apart is the result of [22] where from a pure thermodynamical argument is demonstrated that the transfer should go from DE to DM. See the review [23] for more details and references about interaction models.

This paper is organized as follows: first we present the three interacting models that will be used. In the second part, the data that will constrain these models is explained, as well as the reason why we chose these data and the different combinations in the analysis. In section III we present the analysis and finally, results and discussions.

## II. THE MODELS

In this paper we study the restrictions on interaction models imposed by observational data. Here we study three models of interaction. Explicitly, we study the following cases:

(i)  $Q_1 = 3\gamma H\rho_d,$

(ii)  $Q_2 = 3\gamma H\rho_c,$

(iii)  $Q_3 = 3\alpha H(\rho'_d + \rho'_c),$

where in the last case a prime  $'$  means a derivative with respect to  $\ln a^3$ , with  $a$  being the scale factor. Both (i) and (ii) were already studied in [27]. Model (iii) was studied first in

[31] for the case  $\omega = -1$  and recently in [30]. If  $\gamma$  (or  $\alpha$ ) is zero, then there is no interaction. Also, if  $\gamma < 0$  (or  $\alpha < 0$ ), this indicates that there is transfer of energy from DM to DE.

For the first model (i), the Hubble function  $H(z)/H_0 = E(z)$  is given by

$$E^2(z) = \Omega_m(1+z)^3 + \Omega_r(1+z)^4 + \Omega_d \left( \frac{\gamma}{w+\gamma}(1+z)^3 + \frac{w}{w+\gamma}(1+z)^{3(1+w+\gamma)} \right), \quad (2)$$

where  $\Omega_r = 2.469 \times 10^{-5} h^{-2} (1 + 0.2271 N_{\text{eff}})$  and  $N_{\text{eff}} = 3.04$ , and  $\gamma$  is the parameter that makes the interaction manifest. Here  $\Omega_m = \Omega_c + \Omega_b$ , where  $\Omega_c$  is the non-baryonic part and  $\Omega_b$  is the baryonic one.

For the second model (ii), we obtain

$$E^2(z) = \Omega_d(1+z)^{3(1+w)} + \Omega_r(1+z)^4 + \Omega_b(1+z)^3 + \Omega_c \left( \frac{\gamma}{w+\gamma}(1+z)^{3(1+w)} + \frac{w}{w+\gamma}(1+z)^{3(1-\gamma)} \right). \quad (3)$$

Here the free parameters are  $h$ ,  $\Omega_b$ ,  $\Omega_c$ ,  $w$  and  $\gamma$ . It is clear that for  $\gamma = 0$  both expressions - those for models (i) and (ii) - reduced to that of the  $w$ CDM model.

For the third model (iii) assuming a constant  $\omega$ , we obtain for  $\rho = \rho_c + \rho_d$  the solution

$$\rho(a) = C_1 a^{3\beta^+} + C_2 a^{3\beta^-}, \quad (4)$$

where

$$\beta^\pm = \frac{-2 - (1 - \alpha)w \pm \sqrt{(1 - \alpha)^2 w^2 - 4\alpha w}}{2}, \quad (5)$$

then, the Hubble function can be written as

$$E^2(z) = \Omega_b(1+z)^3 + \Omega_r(1+z)^4 + (1+z)^{-3\beta^+} F_- - (1+z)^{-3\beta^-} F_+. \quad (6)$$

where

$$F_\pm = \frac{\Omega_x(1+w+\beta^\pm) + \Omega_c(1+\beta^\pm)}{\beta^- - \beta^+}. \quad (7)$$

As it is easy to check, turning off the interaction  $\alpha = 0$ , we get from (5) that  $\beta^+ = -1$  and  $\beta^- = -(1+w)$ . Replacing in (7), we get  $F_+ = -\Omega_x$  and  $F_- = \Omega_c$  and (6) reduces to that of the  $w$ CDM model.

### III. THE DATA

In this work, we test the models described in the previous section using 5 types of data: measurements from  $H(z)$ , from type Ia supernova (SNIa), baryonic acoustic oscillations (BAO), gas mass fraction in clusters  $f_{gas}$  and from Cosmic Microwave Background Radiation (CMBR).

Measurements of the Hubble function,  $H(z)$  are taken from several works. They consist of 31 data points compiled in [32] in the range  $z = 0.07$  and  $z = 1.965$ . We have considered points from [33], [34], [35] and also from [36]. We have used only those  $H(z)$  measurements obtained using the differential age method [37], and we have excluded those obtained using the clustering method, because we are also using data from BAO.

The data from SNIa are from the Pantheon sample [24], where the function to be minimized is

$$\chi^2 = (\mu - \mu_{th})^T C^{-1} (\mu - \mu_{th}). \quad (8)$$

Here  $\mu_{th} = 5 \log_{10}(d_L(z)/10pc)$  gives the distance modulus where  $d_L(z)$  is the luminosity distance,  $C$  corresponds to the covariance matrix delivered in [24], and the modular distance is assumed to take the shape

$$\mu = m - M + \alpha X - \gamma Y, \quad (9)$$

where  $m$  is the maximum apparent magnitude in band B,  $X$  is related to the widening of the light curves, and  $Y$  corrects the color. In general, cosmology (specified by  $\mu_{th}$ ) is restricted along with the parameters  $M$ ,  $X$  and  $Y$ . The authors of [24] also deliver a binned sample where only  $M$  is a free parameter.

In addition, we used data from BAO compiled in [38]. This set consists of a sample that combines BAO observations from the 6dF survey [26] at redshift  $z = 0.106$ , with distance measurements from the Sloan Digital Sky Survey (SDSS) data release 7 (DR7), BAO [25] at redshift  $z = 0.15$ , and with data from the Baryon Oscillation Spectroscopic Survey (BOSS) at redshifts  $z = 0.32$ ,  $z = 0.57$  and  $z = 2.34$ . From the observations it is possible to measure the BAO scale in the radial and tangential directions, proving measurements of the Hubble parameter  $H(z)$  and the angular diameter distance  $D_A(z)$  simultaneously.

At low redshift it is not possible to disentangle the BAO scale in the transverse and

line-of-sight directions. The BAO observations give the observed ratios of

$$\frac{D_A(z)}{r_s} = \frac{P}{(1+z)\sqrt{-\Omega_k}} \sin\left(\sqrt{-\Omega_k} \int_0^z \frac{dz}{E(z)}\right), \quad (10)$$

for the transverse direction, where  $r_s$  is the co-moving sound horizon which is independent of  $z$ , and according to Planck it takes the value  $r_s = 1059.68$  [9], and the ratio

$$\frac{D_H(z)}{r_s} = \frac{P}{E(z)}, \quad (11)$$

for the line-of-sight direction. Both in (10) and (11)  $P = c/(r_s H_0)$ , which takes the value  $30.0 \pm 0.4$  for the best  $\Lambda$ CDM Planck fit. This parameter was used in [38] to perform an unanchored BAO analysis, which does not use a value for  $r_s$  obtained from a cosmological constant, also performed in [39].

At low redshift, the surveys give the value for the ratio  $D_V(z)/r_s$ , where

$$D_V(z) = [z(1+z)^2 D_A(z)^2 D_H(z)]^{1/3}, \quad (12)$$

which is an angle-weighted average of  $D_A$  and  $D_H$ . From [38] the data considered are: at low redshift, at  $z = 0.106$  we have  $D_V/r_s = 2.98 \pm 0.13$ , and for  $z = 0.15$ ,  $D_V/r_s = 4.47 \pm 0.17$ . For high redshift we consider  $0.00874D_H/r_s + 0.146D_A/r_s = 1.201 \pm 0.021$  and  $0.0388D_H/r_s - 0.0330D_H/r_s = 0.781 \pm 0.053$  at  $z = 0.32$ ;  $0.0158D_H/r_s + 0.101D_A/r_s = 1.276 \pm 0.011$  and  $0.0433D_H/r_s - 0.0368D_H/r_s = 0.546 \pm 0.026$  at  $z = 0.57$ . Following [38], in order to use the BAO measurements for the Lyman  $\alpha$ , we used the  $\chi^2$  files supplied on the website [40] directly. In what follows, we take the Planck value for  $r_s$  and use  $P$  as a function of  $H_0$ .

We have also used data from gas mass fraction in clusters,  $f_{gas}$  as suggested by [41]. In particular we use the data from [42] which consist in 42 measurements of the X-ray gas mass fraction  $f_{gas}$  in relaxed galaxy clusters in the redshift range  $0.05 < z < 1.1$ . The  $f_{gas}$  data are quoted for a flat  $\Lambda$ CDM reference cosmology with  $h = H_0/100 \text{ km s}^{-1}\text{Mpc}^{-1} = 0.7$  and  $\Omega_m = 0.3$ . To determine constraints on cosmological parameters we use the model function [43]

$$f_{gas}^{\Lambda\text{CDM}}(z) = \frac{b\Omega_b}{(1 + 0.19\sqrt{h})\Omega_M} \left[ \frac{d_A^{\Lambda\text{CDM}}(z)}{d_A(z)} \right]^{3/2}, \quad (13)$$

where  $d_A(z)$  is the angular diameter distance,  $b$  is a bias factor which accounts that the baryon fraction is slightly lower than for the universe as a whole. From [44] it is obtained  $b = 0.824 \pm 0.0033$ . In the analysis we also use standard priors on  $\Omega_b h^2 = 0.02226 \pm 0.0023$

and  $h = 0.678 \pm 0.009$  [45]. It is important to notice that although the data has been produced using the  $\Lambda$ CDM as a reference model, to use this data against other models we have to rebuild the data by dividing by the factor  $d_A^{\Lambda CDM}(z)$  of the equation (13).

Finally we use constraints from measurements of the CMB from the acoustic scale  $l_A$ , the shift parameter  $R$ , and the decoupling redshift  $z_*$ . The  $\chi^2$  for the CMB data is constructed as

$$\chi_{CMB}^2 = X^T C_{CMB}^{-1} X, \quad (14)$$

where

$$X = \begin{pmatrix} l_A - 302.40 \\ R - 1.7246 \\ z_* - 1090.88 \end{pmatrix}. \quad (15)$$

The acoustic scale is defined as

$$l_A = \frac{\pi r(z_*)}{r_s(z_*)}, \quad (16)$$

and the redshift of decoupling  $z_*$  is given by [46],

$$z_* = 1048[1 + 0.00124(\Omega_b h^2)^{-0.738}][1 + g_1(\Omega_m h^2)^{g_2}], \quad (17)$$

$$g_1 = \frac{0.0783(\Omega_b h^2)^{-0.238}}{1 + 39.5(\Omega_b h^2)^{0.763}}, \quad (18)$$

$$g_2 = \frac{0.560}{1 + 21.1(\Omega_b h^2)^{1.81}}, \quad (19)$$

The shift parameter  $R$  is defined as in [47]

$$R = \frac{\sqrt{\Omega_m}}{c(1 + z_*)} D_L(z). \quad (20)$$

$C_{CMB}^{-1}$  in Eq. (14) is the inverse covariance matrix,

$$C_{CMB}^{-1} = \begin{pmatrix} 3.182 & 18.253 & -1.429 \\ 18.253 & 11887.879 & -193.808 \\ -1.429 & -193.808 & 4.556 \end{pmatrix}. \quad (21)$$

Although these priors are obtained using the  $\Lambda$ CDM as a reference model, they can be used to test models not too far from  $\Lambda$ CDM. In fact, as we mentioned in the introduction, in this paper we are studying departures from the concordance model assuming a small coupling between DE and DM, so we expect this constrains being useful to put under stress these interacting models. For more details of the work with the data see [29].

## IV. RESULTS

As we mentioned before, at low redshift it is not possible to disentangle the BAO scale in the transverse and line-of-sight directions, and therefore the surveys report only the average  $D_V$ , usually calibrated using CMB data. At the same time, these low redshift measurements have been consistently in agreement with the  $\Lambda$ CDM model. However, high redshift BAO detection seems to be at variance with the  $\Lambda$ CDM model from nearly  $2.5\sigma$  to  $3\sigma$ . Here, we want to study these effects on three models that present interaction between DE and DM, using not only that for intermediate redshift as  $z = 0.57$ , but also the high redshift ones at  $z = 2.34$  and  $z = 2.36$ . In the latter cases we made use of the entire likelihood provided by the collaboration [40] avoiding the Gaussian approximation used in the literature.

For the analysis we use an Affine-invariant Markov chain Monte Carlo (MCMC) method provided in the **emcee** Python module [48] for the five data sets we have mentioned in the previous section. We consider a burn-in phase where we monitoring the autocorrelation time ( $\tau$ ) and set a target number of independent samples. Then, we set 10000 MCMC steps ( $N$ ) with a number of walkers in the range between 50 and 100. Our estimations of the autocorrelation times for each parameter in the three models all satisfies the relation  $N/\tau \gg 50$  suggested in [48], a condition that is consider a good measure of assets convergence in our samplings.

### A. Model (i)

For this model the free parameters are  $\Omega_c$ ,  $\Omega_b$ ,  $\omega$ ,  $h$  and  $\gamma$ . Although we have performed the analysis for several combinations of data, we presented here only three combinations: A using SNIa+Hz+BAO data, B using SNIa+ $H(z)$ +BAO+ $f_{gas}$ , and C using SNIa+ $H(z)$ +BAO+ $f_{gas}$ +CMB. The best fit of these parameters from our analysis are display in Table I. Using only SNIa data, or combinations like SNIa+ $H(z)$ , or SNIa+ $f_{gas}$  all indicate a preference for zero interaction,  $\gamma \simeq 0$ . In Figure 1, the  $1\sigma$ ,  $2\sigma$  and  $3\sigma$  confidence boundaries for the free parameters of the model (i) are shown, using all the data. According to the Figure, the constraints imposed by the data are consistent with  $\gamma > 0$  – both in the case B and C – indicating positive evidence for an interacting model.



	<i>A</i>	<i>B</i>	<i>C</i>
<i>h</i>	$0.69 \pm 0.02$	$0.687 \pm 0.008$	$0.671^{+0.01}_{-0.008}$
$\Omega_c$	$0.25^{+0.032}_{-0.028}$	$0.293 \pm 0.006$	$0.300 \pm 0.004$
$\Omega_b$	$0.042^{+0.006}_{-0.005}$	$0.047 \pm 0.001$	$0.048 \pm 0.001$
$\omega$	$-1.01^{+0.04}_{-0.06}$	$-1.08 \pm 0.02$	$-1.05 \pm 0.02$
$\gamma$	$0.03^{+0.05}_{-0.06}$	$0.09 \pm 0.01$	$0.07 \pm 0.005$

TABLE I: Best fit values of the cosmological parameters for the interaction model (i) using different data sets. A using SNIa+ $H(z)$ +BAO data. B using SNIa+ $H(z)$ +BAO+ $f_{gas}$ , and C using SNIa+ $H(z)$ +BAO+ $f_{gas}$ + CMB.

### B. Model (ii)

Next, we show the results of our analysis for model (ii). As in the previous case we presented only the results for the same three configurations mentioned. The results are summarized in Table II and also we plot the best fit contours for the case C, with all the data. As we can see, the best fit for this case looks quite similar to the previous one. First of all, there is no clear evidence for interaction in the case of the A set of data, but a positive evidence for interaction – with  $\gamma > 0$  – for the cases B and C. Figure 2 shows the results for the case C.

	<i>A</i>	<i>B</i>	<i>C</i>
<i>h</i>	$0.682^{+0.007}_{-0.009}$	$0.682^{+0.007}_{-0.008}$	$0.669 \pm 0.008$
$\Omega_c$	$0.29 \pm 0.02$	$0.296^{+0.005}_{-0.006}$	$0.301 \pm 0.004$
$\Omega_b$	$0.048 \pm 0.001$	$0.048 \pm 0.001$	$0.049 \pm 0.001$
$\omega$	$-1.01^{+0.03}_{-0.04}$	$-1.02^{+0.04}_{-0.03}$	$-1.03 \pm 0.02$
$\gamma$	$0.004 \pm 0.002$	$0.003^{+0.003}_{-0.002}$	$0.071 \pm 0.006$

TABLE II: Best fit values of the cosmological parameters for the interaction model (ii) using different data sets. The meaning of A, B and C is the same as in Table I.

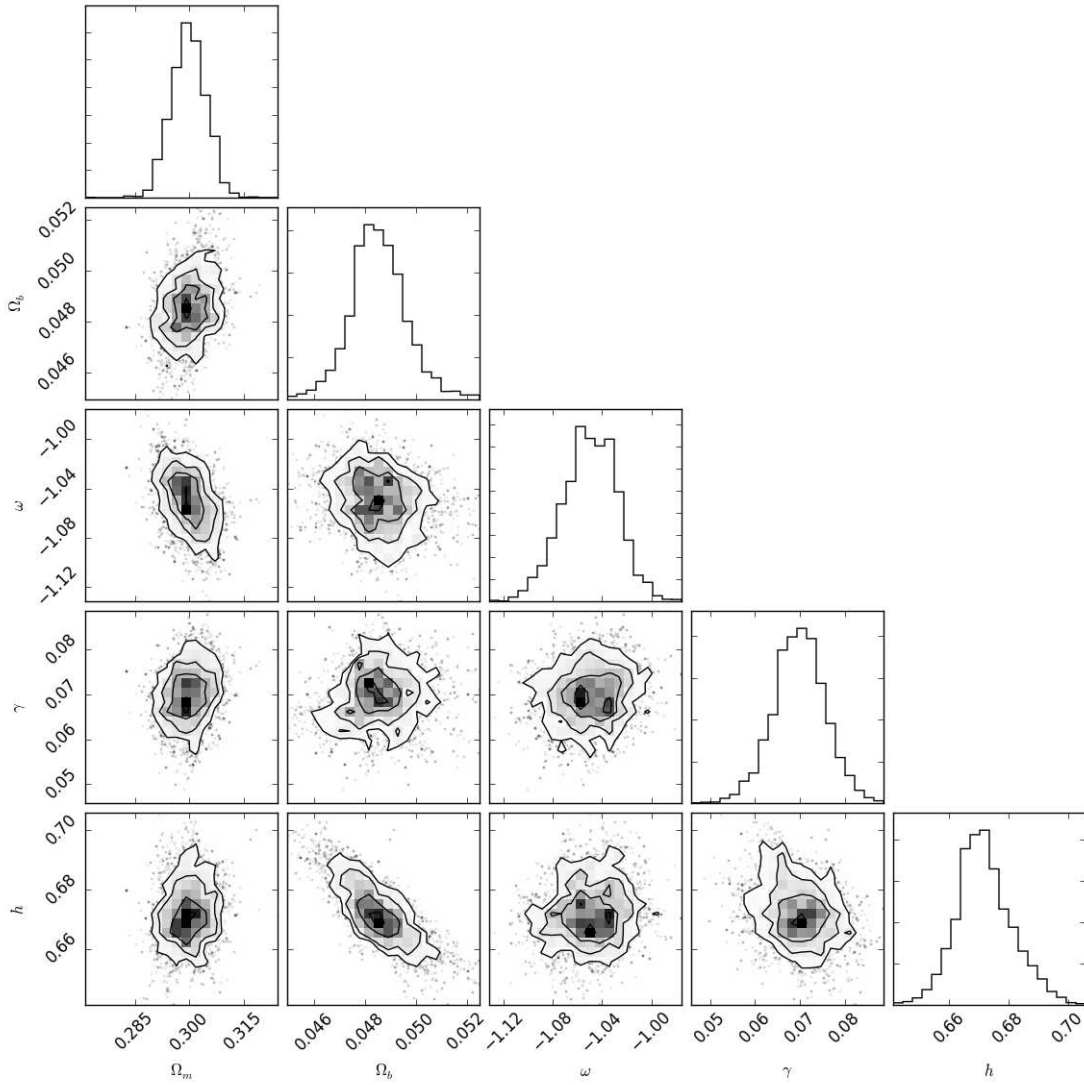


FIG. 1: We display the results for  $1\sigma$ ,  $2\sigma$  and  $3\sigma$  for the model (i) in the parameter space  $(\Omega_m, \Omega_b, \omega, \gamma, h)$  using all the data.

Comparing between Tables I and II, we note that the best fit values of the parameters are essentially the same. In both cases, as we add more data sets, the best fit for  $h$  decreases,  $\Omega_c$  increase,  $\Omega_b$  remains almost fixed, which is expected because of the prior used, the best fit for  $\omega$  is almost the same for each case. Finally for the interaction parameter  $\gamma$ , in the model (i) the best fit remains almost constant as we add more data sets in the analysis, but the uncertainty diminish. In the case of model (ii) the best fit for  $\gamma$  is close to zero for case A and marginally different from zero for case B, but it is definitely not zero for case C. We again observe a non-zero  $\gamma$  using all the data, with a confidence beyond  $3\sigma$ . The rest of the

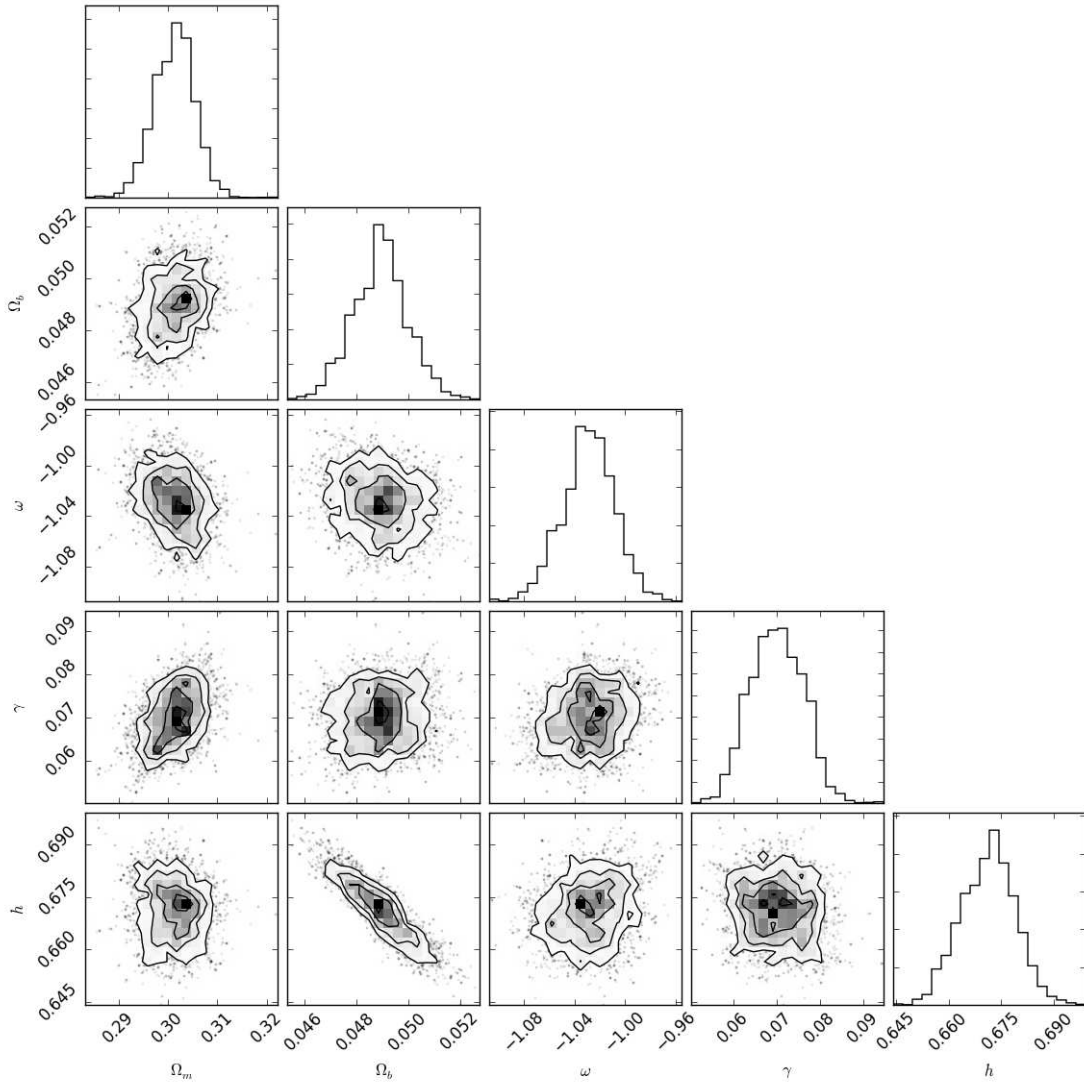


FIG. 2: We display confidence boundaries for  $1\sigma$ ,  $2\sigma$  and  $3\sigma$  for the model (ii) for the free parameters  $(\Omega_m, \Omega_b, \omega, \gamma, h)$  using all the data.

parameters fits values rather similar to that of  $\Lambda$ CDM (Table II). Then, the use of all the data seems to indicate evidence for interaction using model (ii).

### C. Model (iii)

Let us study now the third interacting model. As it is clear from the definition (1), this model is of a different type as those previously studied. The fact that  $Q$  depends on the derivatives of the energy densities, makes it naturally a model more difficult to constraint.

	$D$	$E$	$F$
$h$	$0.69 \pm 0.02$	$0.678 \pm 0.008$	$0.680 \pm 0.009$
$\Omega_c$	$0.36 \pm 0.06$	$0.245 \pm 0.005$	$0.245 \pm 0.006$
$\Omega_b$	$0.046 \pm 0.003$	$0.048 \pm 0.001$	$0.048 \pm 0.001$
$\omega$	$-1.4 \pm 0.2$	$-1.12 \pm 0.06$	$-1.09 \pm 0.04$
$\alpha$	$-0.14 \pm 0.12$	$0.15 \pm 0.06$	$0.11 \pm 0.03$

TABLE III: Best fit values of the cosmological parameters for model (iii) using different data sets. The meaning of  $D$  is for the combination SNIa+ $H(z)$ , for  $E$  the combination SNIa+ $f_{gas}$  and for  $F$  the combination SNIa+ $H(z)$  +  $f_{gas}$

This observation is also supported by the form of the solution (6) compared to the previous ones. As we mention for model (i), we have also performed the analysis using only SNIa data, or combinations like SNIa+ $H(z)$ , SNIa+ $f_{gas}$  or SNI+ $H(z)$ +BAO. Because it is interesting to discuss these results, we display the best fit values in Table III.

	$A$	$B$	$C$
$h$	$0.70 \pm 0.02$	$0.70 \pm 0.02$	$0.69 \pm 0.02$
$\Omega_c$	$0.37^{+0.05}_{-0.06}$	$0.37 \pm 0.06$	$0.31^{+0.06}_{-0.05}$
$\Omega_b$	$0.045^{+0.03}_{-0.02}$	$0.045 \pm 0.002$	$0.046^{+0.002}_{-0.003}$
$\omega$	$-1.4 \pm 0.2$	$-1.4^{+0.2}_{-0.3}$	$-1.2 \pm 0.2$
$\alpha$	$-0.1 \pm 0.1$	$-0.15^{+0.13}_{-0.14}$	$0.0 \pm 0.1$

TABLE IV: Best fit values of the cosmological parameters for model (iii) using different data sets. The meaning of A, B and C is the same as in Table 1.

As can be see there, in the case D where the data used is the combination SNIa+ $H(z)$ , the interaction parameter  $\alpha$  seems to be centered at a negative value ( $\gamma < 0$ ), at least at  $1\sigma$ . The rest of the parameters are not too far from those of  $\Lambda$ CDM except  $\Omega_c$  that has clearly a higher value. For the case E – using the combination SNIa+ $f_{gas}$  – the interaction parameter  $\alpha$  shows a clear tendency for a positive value, and different from zero even at

$3\sigma$ . The rest of the parameters are those typically of the  $\Lambda$ CDM. Finally, for the case F – using the combination SNIa+ $H(z)$  +  $f_{gas}$  – the results are almost similar to those of case E, finding evidence at  $3\sigma$  for a positive value of  $\alpha$  with the rest of the parameters similar to the  $\Lambda$ CDM model.

Adding the BAO data to the previous case, the best fit results change a lot. First of all, the best fit of the interaction parameter  $\alpha$  moves to a negative value, at least to  $1\sigma$ . The value for  $\Omega_c$  increases its value but increase also its uncertainty. The  $\omega$  parameter moves to a more negative value at  $3\sigma$  from the  $\Lambda$ CDM value  $-1$ . All these results are shown in

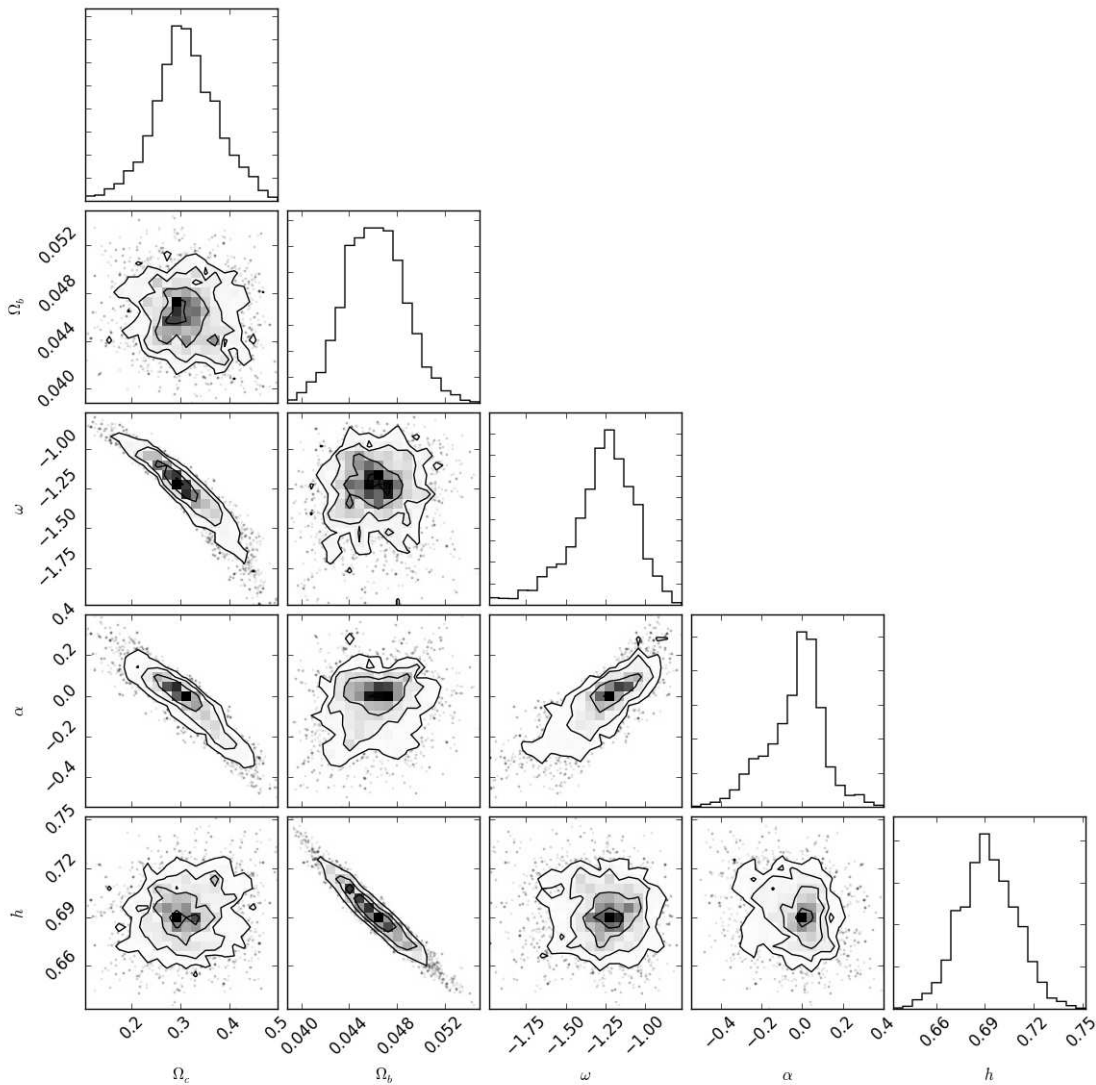


FIG. 3: We display confidence boundaries for  $1\sigma$ ,  $2\sigma$  and  $3\sigma$  for model (iii) for the free parameters  $(\Omega_c, \Omega_b, \omega, \alpha, h)$  using all the data.

the second column (case B) of Table IV. The first column, the case A for the combination SNIa+ $H(z)$ +BAO shows almost the same values as that of case B. However, the case C, the one with all the data shows clearly no evidence for interaction, while the rest of the parameters are typically those from the  $\Lambda$ CDM model.

## V. DISCUSSION

We reported the results of analyzing three interaction models between DE and DM, using five observational probes: type Ia supernova,  $H(z)$  measurements, BAO data, gas mass fraction in clusters data  $f_{gas}$  and CMBR data. In particular we use the BOSS BAO measurements at  $z \simeq 0.32, 0.57$  and  $2.34$ , using the full 2-dimensional constraints on the angular and line of sight BAO scale. Using the combination of all the data, the models (i) and (ii) show positive evidence for the existence of an interaction already at  $1\sigma$  – see Figures (1), and (2)) – and extended up to  $3\sigma$ , implying a transfer of energy from DE to DM, as thermodynamics considerations seems to indicate [22], [23]. However, as we mentioned in the last section for model (iii), using all the data there is no evidence for interaction (see Fig.(3)).

Although we have used prior for  $h$  and  $\Omega_b h^2$  and with it, the best fit parameters tend to take values similar to those of the  $\Lambda$ CDM, in the case of models (i) and (ii) the evidence is clear for a preference of an interacting model with  $\gamma > 0$  that translate in  $Q > 0$  indicating a transfer of energy from DE to DM.

Although this study does not incorporate dynamical constraints, such as those from perturbations, our results seem to indicate a chance to find evidence for a non-zero interaction term in the recent cosmological evolution. A work on this topic is under development.

- 
- [1] A. G. Riess *et al.* [Supernova Search Team], *Astron. J.* **116**, 1009 (1998) [astro-ph/9805201].
  - [2] S. Perlmutter *et al.* [Supernova Cosmology Project Collaboration], *Astrophys. J.* **517**, 565 (1999) [astro-ph/9812133].
  - [3] P. J. E. Peebles and B. Ratra, *Astrophys. J.* **325**, L17 (1988).
  - [4] B. Ratra and P. J. E. Peebles, *Phys. Rev. D* **37**, 3406 (1988).
  - [5] C. Wetterich, *Nucl. Phys. B* **302**, 668 (1988).

- [6] A. Joyce, L. Lombriser and F. Schmidt, *Ann. Rev. Nucl. Part. Sci.* **66**, 95 (2016)
- [7] S. Weinberg, *Rev. Mod. Phys.* **61**, 1 (1989).
- [8] S. M. Carroll, W. H. Press and E. L. Turner, *Ann. Rev. Astron. Astrophys.* **30**, 499 (1992).
- [9] Planck Collaboration, P.A.E. Ade et al., *Astron. Astrophys.* **594**, A13 (2016).
- [10] E. Di Valentino, A. Melchiorri and J. Silk, *Phys. Rev. D* **92**, no. 12, 121302 (2015).
- [11] L. Amendola, *Phys. Rev. D* **62**, 043511 (2000)
- [12] W. Zimdahl and D. Pavon, *Phys. Lett. B* **521**, 133 (2001) doi:10.1016/S0370-2693(01)01174-1 [astro-ph/0105479].
- [13] L. P. Chimento, A. S. Jakubi, D. Pavon and W. Zimdahl, *Phys. Rev. D* **67**, 083513 (2003) doi:10.1103/PhysRevD.67.083513 [astro-ph/0303145].
- [14] S. del Campo, R. Herrera, G. Olivares and D. Pavon, *Phys. Rev. D* **74**, 023501 (2006) doi:10.1103/PhysRevD.74.023501 [astro-ph/0606520].
- [15] V. Salvatelli, N. Said, M. Bruni, A. Melchiorri and D. Wands, *Phys. Rev. Lett.* **113** (2014) 18, 181301.
- [16] B. Wang, C. Y. Lin, D. Pavon and E. Abdalla, *Phys. Lett. B* **662**, 1 (2008)
- [17] E. Abdalla, L. R. W. Abramo, L. Sodre, Jr. and B. Wang, *Phys. Lett. B* **673**, 107 (2009)
- [18] W. Yang, S. Pan, E. Di Valentino, R. C. Nunes, S. Vagnozzi and D. F. Mota, arXiv:1805.08252 [astro-ph.CO].
- [19] C. G. Boehmer, G. Caldera-Cabral, R. Lazkoz and R. Maartens, *Phys. Rev. D* **78**, 023505 (2008)
- [20] S. Kumar and R. C. Nunes, *Phys. Rev. D* **96**, no. 10, 103511 (2017)
- [21] S. Pan and G. S. Sharov, *Mon. Not. Roy. Astron. Soc.* **472**, no. 4, 4736 (2017)
- [22] D. Pavon and B. Wang, *Gen. Rel. Grav.* **41**, 1 (2009)
- [23] B. Wang, E. Abdalla, F. Atrio-Barandela and D. Pavon, *Rept. Prog. Phys.* **79**, no. 9, 096901 (2016) [arXiv:1603.08299 [astro-ph.CO]].
- [24] D. M. Scolnic *et al.*, doi:10.17909/T95Q4X arXiv:1710.00845 [astro-ph.CO].
- [25] A. J. Ross, L. Samushia, C. Howlett, W. J. Percival, A. Burden and M. Manera, *Mon. Not. Roy. Astron. Soc.* **449**, no. 1, 835 (2015) [arXiv:1409.3242 [astro-ph.CO]].
- [26] F. Beutler et al., *MNRAS*, 416, 3017, 2011
- [27] D. Xia, S. Wang, *MNRAS* **463**, 952-956 (2016)
- [28] Planck Collaboration, *Astron. and Astrophys.* 594, A13 (2016).

- [29] V. H. Cardenas, Phys. Lett. B **750**, 128 (2015)
- [30] G. S. Sharov, S. Bhattacharya, S. Pan, R. C. Nunes and S. Chakraborty, Mon. Not. Roy. Astron. Soc. **466**, no. 3, 3497 (2017) [arXiv:1701.00780 [gr-qc]].
- [31] L.P. Chimento, Phys. Rev. D **81**, 043525 (2010)
- [32] J. Magana, M. H. Amante, M. A. Garcia-Aspeitia and V. Motta, Mon. Not. Roy. Astron. Soc. **476**, 1036 (2018)
- [33] C. Zhang et al., Res. Astron. Astrophys. **14**, 1221 (2014).
- [34] D. Stern, R. Jimenez, L. Verde, M. Kamionkowski, and S.A. Stanford, JCAP **1002**, 008 (2010).
- [35] M. Moresco *et al.*, JCAP **1208**, 006 (2012).
- [36] M. Moresco, Mon. Not. Roy. Astron. Soc. **450**, no. L16 (2015).
- [37] R. Jimenez and A. Loeb, Astrophys. J. **573**, 37 (2002).
- [38] J. Evslin, JCAP **1704**, 024 (2017) [arXiv:1604.02809 [astro-ph.CO]].
- [39] E. Aubourg et al., Phys. Rev. D **92**, 123516 (2015).
- [40] <http://darkmatter.ps.uci.edu/baofit/>
- [41] S. Sasaki, Publ. Astron. Soc. Jap. **48**, L119 (1996).
- [42] S. W. Allen, D. A. Rapetti, R. W. Schmidt, H. Ebeling, G. Morris and A. C. Fabian, Mon. Not. Roy. Astron. Soc. **383**, 879 (2008) [arXiv:0706.0033 [astro-ph]].
- [43] S. W. Allen, R. W. Schmidt, H. Ebeling, A. C. Fabian and L. van Speybroeck, Mon. Not. Roy. Astron. Soc. **353**, 457 (2004) [astro-ph/0405340].
- [44] V. R. Eke, J. F. Navarro and C. S. Frenk, Astrophys. J. **503**, 569 (1998) [astro-ph/9708070].
- [45] M. Tanabashi et al. (Particle Data Group), Phys. Rev. **D 98**, 030001 (2018).
- [46] W. Hu and N. Sugiyama, Astrophys. J. **471**, 542 (1996).
- [47] J.R. Bond, G. Efstathiou, M. Tegmark, Mon. Not. Roy. Astron. Soc. **291**, L33 (1997).
- [48] D. Foreman-Mackey, D.W. Hogg, D. Lang, and J. Goodman, Publications of the Astronomical Society of the Pacific, **125**, 306 (2013).